Optimal Tyre Management for a High-Performance Race Car

W.J. West[a] and D.J.N. Limebeer[b]

[a]Department of Electrical, Electronic and Computer Engineering, University of Pretoria, Pretoria, South Africa (Email: wilhelm.west@tuks.co.za); [b]Department of Electrical and Electronic Engineering Science, University of Johannesburg, Johannesburg, South Africa (Email: david.limebeer@gmail.com).

ABSTRACT
Optimal control is used to study the management of tyre performance for a Formula One car. Tyre friction is compromised by accumulated wear and operation outside the tyre design temperature window—inappropriate thermal operation accelerates tyre wear. In this study tyre wear is modelled as a function of the tyre surface temperature and the power dissipated at the road contact. The tyre's frictional performance is modelled as a function of temperature and accumulated wear. A previously developed thermodynamic model is modified by the addition of a state representing the tyres' carcass temperature. Optimal control calculations are used to optimise (multi-lap) performance by improving grip and extending the life of the tyres. In combination, tyre wear and friction control can be used to schedule tyre changes and minimise race times.

1. Introduction

A critical facet of race strategy is tyre management. The aim of this paper is to show how tyre management can be enhanced by optimal control. The study presented here builds on the work in [1,2]. Since tyre friction and wear are both sensitive to temperature, a representative model of the tyres' thermal behaviour is introduced. It is also necessary to couple the tyres' operating temperature to its friction and wear characteristics. Tyre-focussed research has shown that the friction properties of tyre rubber are influenced by a number of factors including the tyre compound, track roughness, tyre loading, and the rubber temperature [3]. Of particular import is the fact that tyre wear reduces the available friction, and consequently erodes the vehicle's long-stint race performance [4].

There is now substantial evidence to support a 'two-mechanism' theory of rubber abrasion [5]. The first predominates when the tread rubber experiences elastic surface deformations induced by frictional contact with road asperities. Under these conditions rubber particles are removed from the tread by a tensile tearing process. The second mechanism predominates when the rubber experiences a plastic contact with road asperities. This contact exists on a smaller scale and particles are removed by an abrasive-cutting action. The first mechanism is favoured by higher temperatures,

low microtexture road surfaces, and soft tyre compounds. The second mechanism predominates at lower temperatures, on high microtexture road surfaces, and with harder tyre compounds.

The review article [6] discusses rubber abrasion, as well as the associated underlying theory and experiments. At moderate slip, wear increases as the square of the slip, and at constant slip, wear increases with increasing rubber stiffness, and decreases with increasing elastic hysteresis. Theoretical work presented in [7] is validated with a thin rigid wheel experiment. It is shown that at low slip the wear-rate is given by

$$\dot{w} = \frac{\gamma r f^2}{c};$$ (1)

$\dot{w}$ is the volumetric of wear rate, γ represents the rubber's abradibility, r is the test wheel radius, f is the lateral force, and c is a measure of the wheel's stiffness. An example of a similar experimentally derived formula is available in the FTire model [8]. Care must be taken when considering the application of laboratory results based on solid wheels to real road tyres. The stiffness c in (1) refers to a rigid wheel, while in road tyre rigidity is dominated by the flexibility of the pneumatic chamber, the carcass, and the tread.

The influence of temperature is discussed in [6]. Their Figure 5 shows that the rubber abradibility increases at both low and high temperatures—this leads immediately to the idea that the tyre rubber's abradibility should be made a function of temperature. It also supports the 'two-mechanism' theory of rubber abrasion. As explained in [9], strong wear may occur at low temperatures where the rubber behaves as a glassy brittle material, and where the rubber can fracture by crack propagation. At sliding velocities typical of a braking wheel, one expects large wear, with rubber particles being removed by brittle fracture. During sliding the road asperities exert oscillatory shear stresses on the tyre rubber, and at higher temperatures these shear stresses may break molecular bonds within the tread base material. This stress-assisted thermally-activated bond breaking gives rise to a rapid increase in high-temperature wear. The 'two-mechanism' theory of rubber abrasion leads us to expect a U-shaped wear characteristic of the form illustrated in Figure 1.
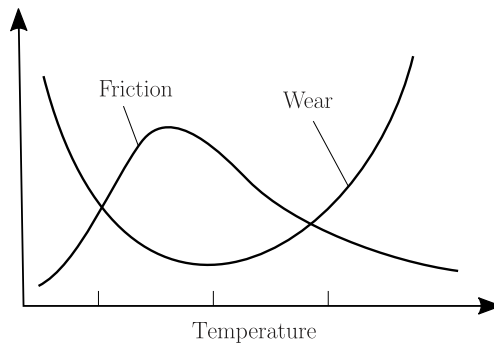

Figure 1. Temperature dependence of rubber friction and wear [9]; based on experimental results in [10].

The wear model used here follows [2], which is reminiscent of (1) in the optimum temperature operating range. It is important to note that wear is minimised at temperatures close to those associated with maximum friction. The optimal temperature range tends to be a narrow one with high-performance race tyres; see [2] and the references therein.

2

In previous work optimal control simulations have been used to tailor vehicle set-up parameters for specific tracks, cater for three-dimensional tracks, as well as refine race strategy [11–13]. These simulations did not take account for tyre temperature or wear, and were restricted to single-lap studies. In [1,2] thermodynamic models were developed, where grip was modelled as a function of tread temperature. The wear model in [2] highlights the trade-off between lap times and tyre wear. The long-term performance impact of tyre wear has not as yet been considered in any detail, and is the focus of this paper.

The thermodynamic model developed in [2] is extended to include a tyre carcass temperature state. This enhancement is introduced in order to better represent the tyre surface temperature behaviour. As an important and novel feature, grip is modelled as a function of tyre wear in order to recognise the long-run impact of tyre degradation. The enhanced model is incorporated into a multi-lap simulation in order to evaluate the performance impact of tyre wear over a multi-lap racing stint. It is hoped that this study will assist racing teams to develop improved tyre management strategies.

Section 2 addresses the tyre modelling, including thermal, friction, and wear behaviours. The general influences of tyre temperature and wear are outlined in Section 2.1. The thermodynamics of the tyre is modelled in Section 2.2. Tyre model parameter fitting is described in Section 2.3, while the tyre wear model is presented in Section 2.4. A combined temperature–grip characteristic is described in Section 2.5. The track and vehicle modelling is outlined briefly in Section 2.6. Section 3 directs the reader to the numerical optimal control literature that is most relevant to the methods and techniques employed here. The results are given in Section 4, with a track-side example given in Section 5. The conclusions appear in Section 6.
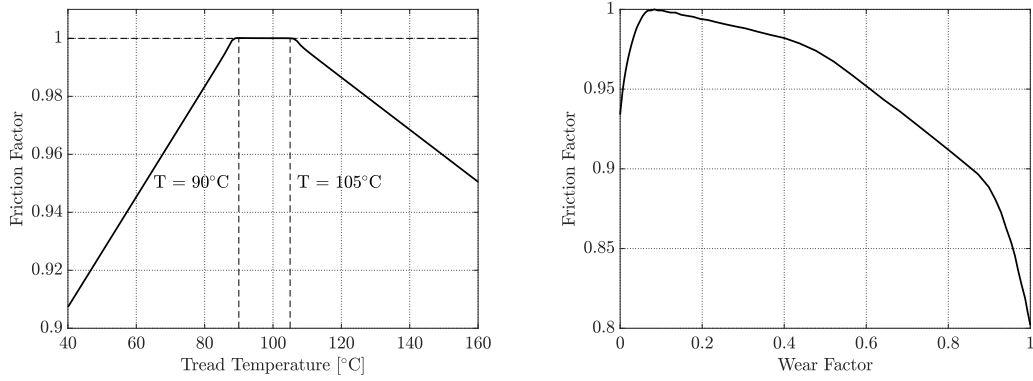
2. Tyre model

The purpose of the tyre model is to reproduce the behaviour of the carcass and tread temperatures, and their influence on grip and tread-wear.

2.1. Overview

Figure 2(a) shows that optimum grip is achieved when the tread temperature lies between 90°C and 105°C; this curve is representative of a super-soft tyre (the compound that will be used for the simulations in the following sections). The optimum temperature operating window will vary between different tyre compounds. The driver's control objective is to get the tyre surface temperatures into this optimal operating window and keep it there as nearly as possible.

Tyre tread temperature variations are reversible, whereas tyre wear is not. To study tyre management, the tyre model must reproduce the mechanisms that lead to wear and the associated irreversible degradation. Examples of how different tyre types lose performance are described in [4]; see Figure 2 therein. Passenger tyres are typically designed for longevity, whereas racing tyres are designed to offer enhanced grip for a shorter time. The wear curve for a performance tyre compound is shown in Figure 2(b). The grip initially increases with use before it begins to degrade; racing tyres are not fully vulcanised during the manufacturing process [14]. During the initial wear phase the rubber goes through a curing process that forms cross-links between sections of the rubber polymer chains. This curing process increases the grip, rigidity and durability of the tyre [15].

(a) Optimal temperature window for super-soft tyre compound.

(b) Wear characteristics of a racing tyre compound [4].

Figure 2. Optimal temperature window and wear characteristic for a super-soft tyre compound.

Several thermodynamic tyre models have already appeared in the literature. These range from complex finite element representations [16] and its descendants, to relatively simple lumped parameter models [1,2]. Since these models will be used in optimal control calculations, a simple thermal model is preferred. The tread-only model used in [2] is limited by the fact that it exaggerates the extent to which it is possible to cool the tread once it overheats. Once the tread overheats, reducing the temperature of the tyre carcass becomes necessary—this process is slowed by the relatively high thermal inertia of the carcass as compared to that of the tyre tread. It is thus important to introduce a carcass temperature state that represents this thermal-inertia-related lag. In a typical race the tread will undergo rapid temperature variations throughout a racing lap, while the carcass temperature varies much more slowly. The model in [1] comprises of three states: the tread temperature, the carcass temperature, and the inflation gas temperature. Their results show that the tread temperatures increase rapidly under braking and turn entry, and then decays in an exponential manner on high-speed sections. Important from a modelling perspective is the fact that the dominant heat flows are from the carcass to the tread, and from the tread to the road. Smaller heat flows are associated with the tread to ambient, and the carcass to ambient, with the smallest (and almost negligible) heat flow from the carcass to the gas; see Figure 13 in [1]. For that reason we have not included an inflation gas temperature state in the model presented here. Also, the temperature of the inflation gas was required in [1] to calculate the inflation pressure and the contact patch area. Our tyre model does not need the inflation pressure for this purpose.

2.2. Thermodynamic model

The car tyre thermodynamics are modelled using tyre-carcass and tyre-surface temperature states—this is an extension of the model proposed in [2]. In recognition of a warning originally due to Enrico Fermi, the number of free model parameters has been reduced[1]. The track temperature and the ambient temperature of the surrounding air are treated as constant. The tyre-surface temperature state is associated with the tread. The tyre's carcass temperature state is used to represent the temperature of the tyre's bulk material including the core and side-wall rubber, and the metal struc-

---

[1] 'With four parameters I can fit an elephant, and with five I can make him wiggle his trunk [17].'

ture that provides the tyre with its basic shape and mechanical strength. The high thermal conductivity of the metal structure lends support to the isotropic modelling assumption. Figure 3 shows the main components of the lumped parameter model used to describe the thermodynamic behaviour of the tyres.
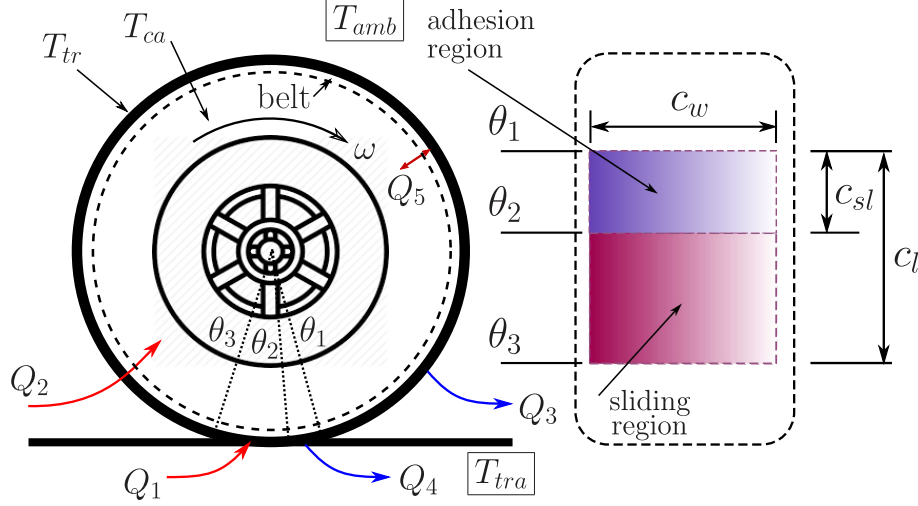

Figure 3. Thermodynamic model with dominant heat flows

The tyre model comprises four temperatures and five heat flows as detailed in Table 1. We will assume that: (i) Q_1 is generated by tyre slip, (ii) Q_2 is generated by flexing of the tyres' structure and carcass, (iii) Q_3 is heat lost by convective cooling, (iv) Q_4 represents heat lost by conductive cooling in the adhesion region of the contact patch, and (v) Q_5 represents the heat transfer between the tread and the carcass. The lumped parameter model used in [2] represents the thermal behaviour of racing tyres during single-lap simulations only.

Table 1. Tyre temperatures and heat flows

Item	Description
T_{amb}	Ambient temperature (asssumed fixed)
T_{tra}	Track temperature (asssumed fixed)
T_{tr}	Tread temperature
T_{ca}	Carcass temperature
Q_1	heat generated in the tyre sliding region
Q_2	heat generated due to tyre carcass deflection
Q_3	heat loss due to convective cooling
Q_4	conductive cooling in the adhesion region of the contact patch
Q_5	heat flow between the tread and the carcass

The prior model [2] is expanded by adding a carcass temperature state, with its associated heat transfer equation. The differential equations for the tyre tread temperature, T_{tr}, and the tyre carcass temperature, T_{ca}, are obtained by simple energy balances:

$$m_t c_t \frac{\mathrm{d}}{\mathrm{d}t} T_{tr} = Q_1 - Q_3 - Q_4 + Q_5 \tag{2}$$

$$m_c c_c \frac{\mathrm{d}}{\mathrm{d}t} T_{ca} = Q_2 - Q_5; \tag{3}$$

m_t and m_c are the tread and carcass masses, and c_t and c_c are respectively the tread and carcass specific heat capacities.

The heat generated in the contact patch is calculated by summing the longitudinal and lateral slip powers:

$$Q_1 = p_1 u_n (|F_x \kappa| + |F_y \tan \alpha|). \tag{4}$$

The tunable parameter p_1 represents the portion of frictional power that goes to heating the tread. The slip quantities α and κ, and the tyre forces F_x and F_y are calculated using formulae given in Appendix 2 in [2]. The longitudinal velocities u_n of each wheel are given by equations (3) to (6) in [2]. The car parameters are given in Table A1 of [2].

As the wheels rotate, the carcass undergoes cyclic loading and relaxation, which causes the carcass to warm [18]. This type of information can be obtained by direct measurement; see Figure 2 in [16]. Figure 4 shows the stress-strain cycle along with the extreme points A and B.
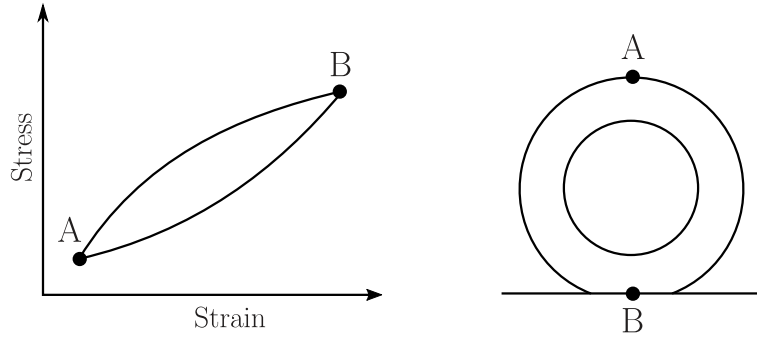

Figure 4. Hysteresis heating and extreme points of stress-strain cycle.

For a given material, the work done per cycle per unit volume, ΔE, corresponds to the area under the hysteresis curve; ΔE is a nonlinear function of the temperature and the inflation-induced initial stress. If the rolling diameter is D, the heating power is of the form $Q_2 = \frac{u_n m_c}{\pi D} \Delta E$. Since the heating process is anisotropic, the tyre carcass deflection heating is represented by

$$Q_2 = p_2 \frac{u_n m_c}{\pi D} \Big(k_1 |F_x| + k_2 |F_y| + k_3 |F_z| \Big), \tag{5}$$

where p_2 is a tunable parameter, and k_1, k_2 and k_3 are used to recognise the anisotropic character of the tyre's construction. The constants k_1, k_2 and k_3 are given in Table 2, while p_2 is fitted to measured track data.

The heat loss due to convection between the tyre tread and the surrounding ambient air is given by:

$$Q_3 = h_{forc} A_{conv} (T_{tr} - T_{amb}), \tag{6}$$

where

$$A_{conv} = A_{tot} - c_w c_l \tag{7}$$

is the area accessible to the ambient air flow. The first term on the right-hand side of (7) is the total surface area of the tread

$$A_{tot} = \pi DW, \tag{8}$$

while the second term is the area of the tread in contact with the road. The tread contact patch widths for the front and rear tyres are given by c_{wf} and c_{wr} respectively; see Table 2.

Table 2. Thermodynamic model parameters

Parameter	Description	Units	Value
T_{amb}	Track air temperature	°C	25
T_{track}	Track surface temperature	°C	35
m_t	Tyre tread mass	kg	0.5
m_c	Tyre carcass mass (front)	kg	9.5
	Tyre carcass mass (rear)	kg	11.5
c_t	Heat capacity of tread	kJ/kg K	2.4
c_c	Heat capacity of carcass	kJ/kg K	1.6
h_{tt}	Track-tyre heat transfer coefficient	kW/m²K	12
c_{wf}	Contact patch width (front)	m	0.20
c_{wr}	Contact patch width (rear)	m	0.22
a_{cp}	Contact patch length constant	m/kN	0.056
α_c	Reference sliding/non-sliding slip angle	°	8
c_{s1}	Sliding/non-sliding reference 1	-	0.3
c_{s2}	Sliding/non-sliding reference 2	-	0.8
k_1	Strain parameter in the x-direction	m	0.1
k_2	Strain parameter in the y-direction	m	0.1
k_3	Strain parameter in the z-direction	m	1.0
D	Tyre diameter	m	0.66
W	Tyre width (front)	m	0.355
	Tyre width (rear)	m	0.380

The lengths of the contact patches c_l are calculated using [2]:

$$c_l = a_{cp} F_z^{0.7}. \tag{9}$$

The heat transfer coefficient h_{forc} is determined using an empirical formula that correlates well with CFD simulation ([16] Equation 10):

$$h_{forc} = \frac{K_{air}}{L} \left[0.0239 \left(\frac{u_n L}{v_{air}} \right)^{0.805} \right]. \tag{10}$$

The conductivity and kinematic viscosity of air, are K_{air} and v_{air} respectively, and are evaluated at the average temperature between the tread and ambient air. Numerical values can be found in material physical property databases—see for example Table A–9 [19]. The characteristic length of the heat exchange surface is given by:

$$L = \frac{1}{1/D + 1/W}, \tag{11}$$

where D is the tyre diameter and W the tread width.

The conductive heat loss from the tyre tread to the track is given by Newton's law of cooling:

$$Q_4 = h_{tt} A_{cp} (T_{tr} - T_{tra}), \tag{12}$$

where h_{tt} is the transfer coefficient of conduction between the track and the tread [1]. The non-sliding area of the contact patch A_{cp} is the given by:

$$A_{cp} = c_w c_s(\alpha) c_l. \tag{13}$$

The function $c_s(\alpha)$ gives the proportion of the contact patch length in the non-sliding region of the tread as the vehicle approaches its cornering limit (see Figure 3)

$$c_s(\alpha) = \frac{\alpha}{\alpha_c}(c_{s2} - c_{s1}) + c_{s1}; \tag{14}$$

c_{s1} and c_{s2} are reference values given in Table 2, while α_c is the reference slip angle.

The heat transfer between the tread and carcass is given by:

$$Q_5 = p_3 A_{tot}(T_{carc} - T_{tread}), \tag{15}$$

where p_3 is a tunable heat transfer coefficient of conduction, and A_{tot} is given in (8).
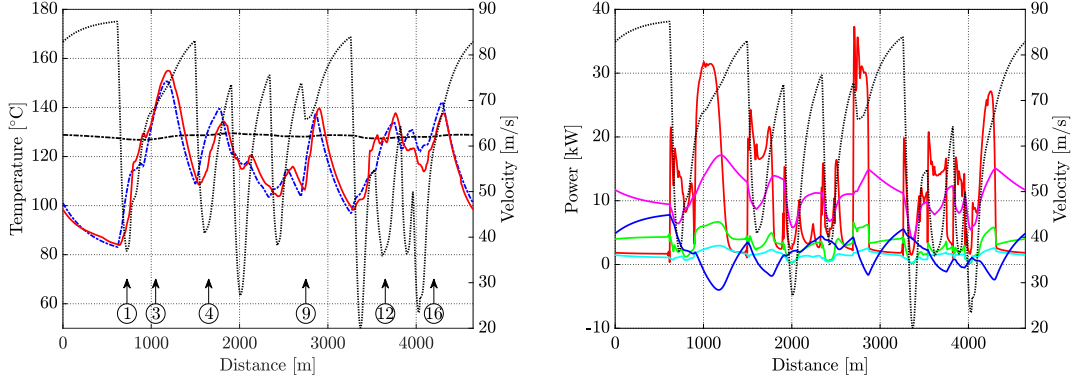
2.3. Parameter fitting

The model parameters were fitted to measured tyre surface temperature data. It is assuming that the tyres were at operating temperatures and that the car was driving multiple laps. Matching tyre carcass temperature data would be highly desirable, but this information was not available. Measured data of this type can be reviewed in Figure 8 of [16]. For that reason the tread and carcass temperatures were constrained to be cyclic in the parameter optimisation process. Figure 5(a) shows a best-fit parameter set for the rear-left tyre, which has a root mean square error of 5.6°C. The associated heat flows are shown in Figure 5(b). Similar plots were obtained for the other tyres, but these are not shown here. No telemetry data was available for the carcass temperature, which varies relatively slowly. The slow carcass temperature behaviour is attributable to its greater thermal inertia as compared to the thin tread layer. In essence, the carcass acts as a heat store that prevents the tread from cooling down to the track temperature. Table 3 shows the parameters that resulted in the best fit for each tyre.

Table 3. Thermodynamic tyre model parameters

Parameter	Front left	Front Right	Rear left	Rear right
p_1	0.6687	0.6836	0.4924	0.5861
p_2	0.0	0.1484	0.1802	0.1254
p_3	196.61	311.21	222.17	182.11

The rear-left tread and carcass temperatures begin a high-speed lap at approximately at 100°C, which is within the optimal operating temperature range; see Figure 2(a). The tread then cools on the high-speed straight of approximately 750 m before the car enters turn 1. On this initial section the tyre experiences very little sliding friction Q_1, modest deflection heating Q_2, significant, but decreasing convective cooling Q_3, almost no conductive cooling Q_4, and an increasing level of heat transfer to the rapidly cooling tread Q_5. The car then slows on the entry to turn 1, and the tread begins to heat up under firm braking due to increased Q_1. There is a decrease in the deflection heating Q_2 due to reduced wheel speed, the convective heating Q_3 reduces,

(a) Tread and carcass temperature. Car speed (dotted), tread temperature telemetry data (red), model tread temperature (blue), model carcass temperature (dot-dash); the locations of some corners circled.

(b) Heat flows. The car speed (dotted), Q_1 (red), Q_2 (green); Q_3 (magenta); Q_4 (cyan); Q_5 (blue).

Figure 5. Parameter fitting using telemetry data for the rear-left tyre for one lap of Circuit de Catalunya.

the conductive cooling Q_4 remains small, and the heat transfer between the tread and carcass Q_5 reduces. The car then accelerates into the high-speed turn 3. Under firm acceleration and high lateral force loads, the rear-left tyre experiences over 30 kW of friction heating Q_1, the deflection heating Q_2 increases, as the speed increase, and the convection cooling Q_3 increases too–equation (10) is a function of speed. The conductive cooling Q_4 remains small, while Q_5 sees an increase. Towards the end of turn 3 the tread temperature increases to approximately 150°C. The tyre then cools on the straight leading to turn 4. Further heating occurs on the entry to turn 4, with the tyre then cooling again on the straight between turns 4 and 5. Another temperature peak of approximately 140°C occurs under braking in turn 9. The tread temperature behaviour for the remainder of the lap can be explained in much the same way. As expected, the tread temperature varies rapidly, while the carcass temperature varies much more slowly.

2.4. Tyre wear model

The model developed in [2] forms the basis of this aspect of the work. The wear rate $(\dot{w})$ is added as an extra state to be associated with each tyre, so that the total tyre wear can be calculated. The mechanical abrasion between a tyre and track asperities is modelled using the power law relationship:

$$\dot{w}_p = w_{p1}\Big(\frac{Q_1}{Q_{ref}}\Big)^{w_{p2}}, \qquad (16)$$

where Q_1 is given in (4), and w_{p1}, w_{p2} and Q_{ref} are constants; see Table 4. If a tyre is overworked while cold, particles break away from the surface (in a phenomenon known as 'graining'), which is modelled by[2]:

---

[2]Most optimal control solvers using nonlinear programmes cannot deal with 'nonsmooth' functions. To that end, a smooth approximation to (17) is

$$\dot{w}_g = w_{g1}\left((T_{tp} - T_{tr} + \sqrt{(T_{tp} - T_{tr})^2 + \epsilon})/2\right)^{w_{g2}}$$

9

$$\dot{w}_g = w_{g1}(\max(T_{tp} - T_{tr}, 0))^{w_{g2}}; \tag{17}$$

w_{g1} and w_{g2} are constants; see Table 4. The wear transition temperature is in the optimal grip temperature range; see Figure 2(a). If a tyre gets too hot, local hot spots will form leading to more extreme tyre wear. This phenomenon is commonly called 'blistering' and is modelled by[3]:

$$\dot{w}_b = w_{b1}(\max(T_{tr} - T_{tp}, 0))^{w_{b2}}, \tag{18}$$

in which w_{b1} and w_{b2} are constants. As is apparent from (17) and (18), these wear mechanisms occur either side of the optimum wear temperature T_{tp}. In combination, (17) and (18) represent the 'two-mechanism' abrasion that occur either side of the optimal operating temperature.

Table 4. Tyre wear model parameters

Parameter	Description	Units	Value
w_{p1}	Frictional power gain factor	mm/s	0.09
w_{p2}	Frictional power exponent	—	1.6
Q_{ref}	Reference frictional power	kW	150
w_{g1}	Graining gain factor	mm/°C s	0.4×10^{-5}
w_{g2}	Graining exponent	—	2
T_{tp}	Wear transition temperature	°C	100
w_{b1}	Blistering gain factor	mm/°C s	0.8×10^{-5}
w_{b2}	Blistering exponent	—	2

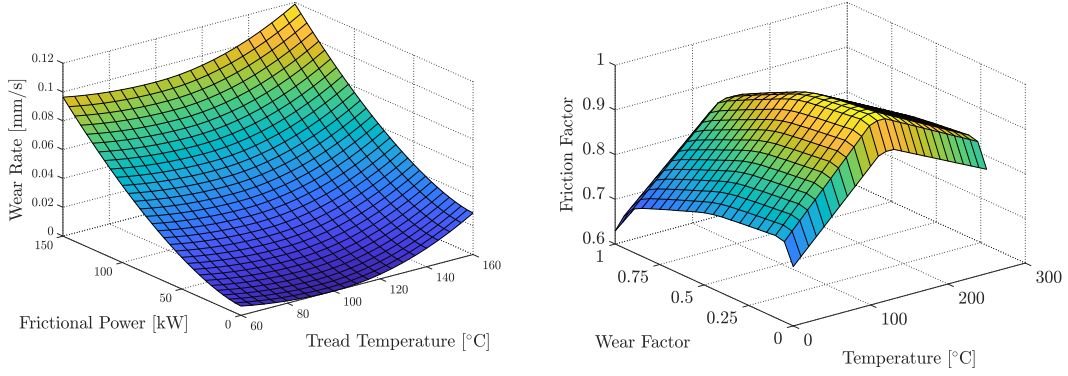### 2.5. Combined temperature–grip characteristic

The total tyre wear is found by integrating the superposition of the three wear rate mechanisms given in (16), (17) and (18). The combined wear rate is illustrated in Figure 6(a). In order to complete the tyre model, we will combine the tyre wear with the temperature characteristic illustrated in Figure 2(a). This leads to a grip factor characteristic, which is a function to both temperature and wear. This allows the tyre grip to be modelled as a function of the tread temperature (a reversible process), and tyre wear (an irreversible process). As a result, the tyres can be managed by the optimal control process until they can be replaced at scheduled pit stops. The three-dimensional grip-sensitivity curve used in this study is shown in Figure 6(b).

Slices along constant wear planes resemble Figure 2(a), whereas slices along constant temperature planes resemble Figure 2(b).

---

for 'small' $\epsilon > 0$. See page 417 [20] for further details.

[3]A usable smooth approximation to (18) is

$$\dot{w}_b = w_{b1}\left((T_{tr} - T_{tp} + \sqrt{(T_{tr} - T_{tp})^2 + \epsilon})/2\right)^{w_{b2}}.$$

(a) Wear rate curve constructed by superimposing equations (16), (17) and (18).

(b) Combined temperature–wear grip curve.

Figure 6. Optimal temperature window and wear characteristic for a super-soft tyre compound.

2.6. Vehicle and track model

The vehicle and track model used here is based on that given in [2,11,12]. The race track is modelled as a flat surface in two dimensions using a curvilinear coordinate system, although a fully three-dimensional track could also be used [13,20]. The distance travelled along the track centreline from the start-finish line is used as the independent variable so that time can be minimised in a fixed-horizon optimal control problem. A rigid body approximation of the car's chassis is used. Longitudinal and lateral forces are produced by the tyres in reaction to the slip angles, longitudinal slips and normal loads. The frictional forces of each tyre is modelled by an empirical relationship that is based on a Magic Formula [21]. These frictional forces are responsive to the tyre's normal loads and combined slip. The vehicle dynamics are modelled by balancing the forces and moments that act on the chassis. The aerodynamic loads consist of downforce and drag, which are dependent on the car's speed. It is assumed that aerodynamic loads are applied at the vehicle's centre of pressure and that the coefficients for downforce and drag remain constant. The interested reader can refer to Appendix A of [2] for a detailed description of the vehicle dynamics. This material is also covered in [20].

3. Optimal control

The use of numerical optimal control to solve minimum-time optimal control problems is covered in several places. The interested reader will find a general overview of numerical optimal control using nonlinear programming in [22]. Applications to several vehicular minimum-time problems are given in [20] and the references therein. Some of the implementation practicalities are also described there. The solution of a closed-circuit minimum-time problem, using GPOPS-II [23], is described in [12]. Predecessor optimal control research, with a focus on tyre management, is described in [2]. In the work described in this paper the objective function of the optimal control problem is to minimise the time taken to complete single, or else multiple laps of the Circuit de Catalunya. As detailed above, these calculations recognise the optimal operating temperature of the tyres as well as tyre wear. While the tyre operating temperature is not constrained directly, minimising the lap time is achieved by maximising grip.

11

This in turn, requires the tyres to operate within their optimal temperature band as much as possible. There is a hard limit of 5 mm on the tread depth of each tyre, but excessive wear will compromise performance and thus be avoided.

4. Results

Simulation results are now given that illustrate the significance of the additions made to the thermal and wear tyre model presented in [2]. These include the introduction of a carcass temperature state, the explicit recognition of tyre wear, and the study of optimal multi-lap racing stints. We will study thermal influences in isolation first, with the effect of wear considered thereafter. This is followed by a sensitivity study that was performed to investigate the effect of track temperature variations on racing performance. We conclude with some track-side observations. The general-purpose optimal control problem solver GPOPS-II is used to perform the optimal control calculations.

4.1. Effect of adding carcass temperature

The optimal control solver is used to minimise the time taken to complete a fifteen-laps stint around the Circuit de Catalunya in Barcelona. The initial carcass and tread temperatures were set to 60°C, which is well below the optimal tyre operating temperature window. A super-soft compound is used that will achieve optimal grip when the tread temperature is between 90°C and 105°C; see Figure 2(a). The temperature profiles for the tyre carcasses are shown in Figure 7(a), while tread temperature of the front-left tread temperature is illustrated in Figure 7(b). The lap ΔT's are also given. As one would expect, the first lap is a relatively slow lap, because the tyres are cold and thus unable to provide optimal grip. During the third lap the rear tyre tread and carcass temperatures increase into the optimal operating range, while the front-right tyre is still running cool. Despite the slightly cool front-right tyre, the second and third laps are the fastest with a lap time of approximately 81.07 s. The positive ΔT values for the other laps indicate that these laps were slower than Laps 2 and 3; these values are shown as the dashed black curves. As the carcasses act as thermal integrators, their temperatures increase slowly over time. However, once the carcasses overheat,
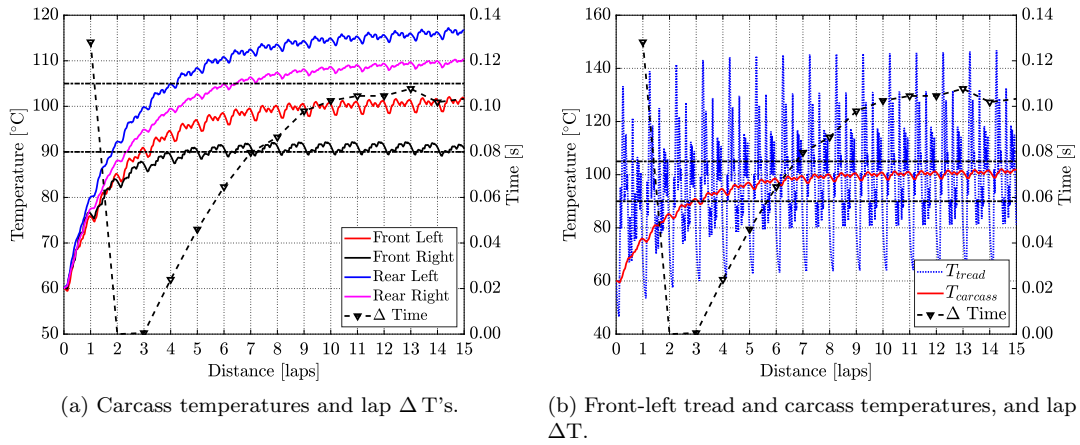

(a) Carcass temperatures and lap Δ T's.

(b) Front-left tread and carcass temperatures, and lap ΔT.

Figure 7. Optimal solution, neglecting tyre wear, for a 15–lap racing stint.

12

it becomes more difficult to keep the tread temperature within the optimal window, and the rear tyres overheat during the second half of the stint. As a result of this overheating, the rear tyres operate sub-optimally, causing a loss of performance in the later laps. The time for Lap 10 increases to 81.17 s, which is only slightly faster than the cold-tyre first lap. As shown in Figure 7(b), the average tread temperature varies rapidly around the corresponding carcass temperature. In the absence of wear-related tyre degradation modelling, identical lap times would be achieved once the tyres are heated up into the desired temperature window [2].

4.2. Influence of tyre wear

To illustrate the influence of tyre wear, a wear acceleration factor is introduced that temporarily exaggerates the effect of wear so that its impact can be studied within a single lap. No wear, nominal wear, 10× nominal wear, and 15× nominal wear cases are considered; in the 15× nominal wear case some tyres are completely worn within a single lap. The tread and carcass temperatures are initially at 60°C, and all the tyre carcasses remain below 83°C, which is below the optimal operating temperature range. With the exception of the front-right tyre, the tyre treads are within the optimal temperature range after 750 m. In the single-lap simulation given in Figure 8, the vehicle speed is not surprisingly fastest in the no-wear reference case. Small speed reductions are observed in the nominal wear and ×10 nominal wear cases. These speed reductions are accompanied by slightly earlier braking, and slightly lower cornering speeds. However, if the wear is increased to ×15 nominal, the race speed falls away significantly and the car becomes uncompetitive.
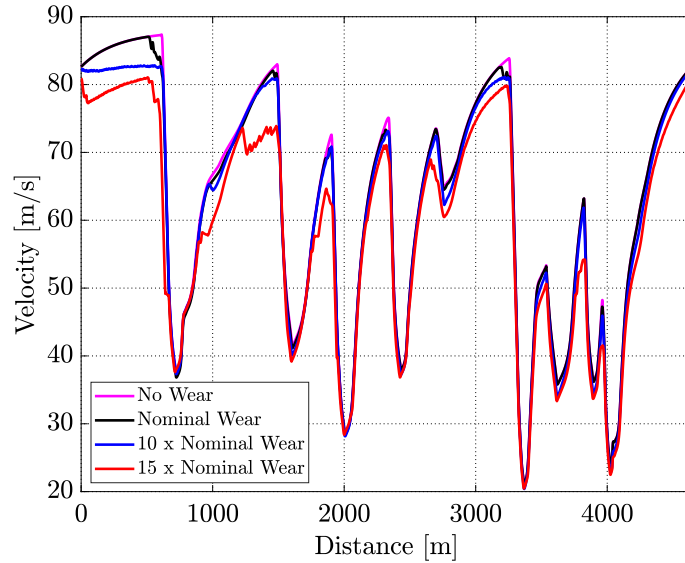

Figure 8. Lap speeds for tyres with temperature effects and varying tyre wear rates.

The reason for this is evident in Figure 9, which shows that in the ×15 nominal case, and despite optimal tyre management, both front tyres are worn out by the end of the lap (the new tread is assumed to be 5 mm thick). In the ×10 nominal case the front tyres are heavily worn, but this has not as yet had a catastrophic effect on the car's performance.

13

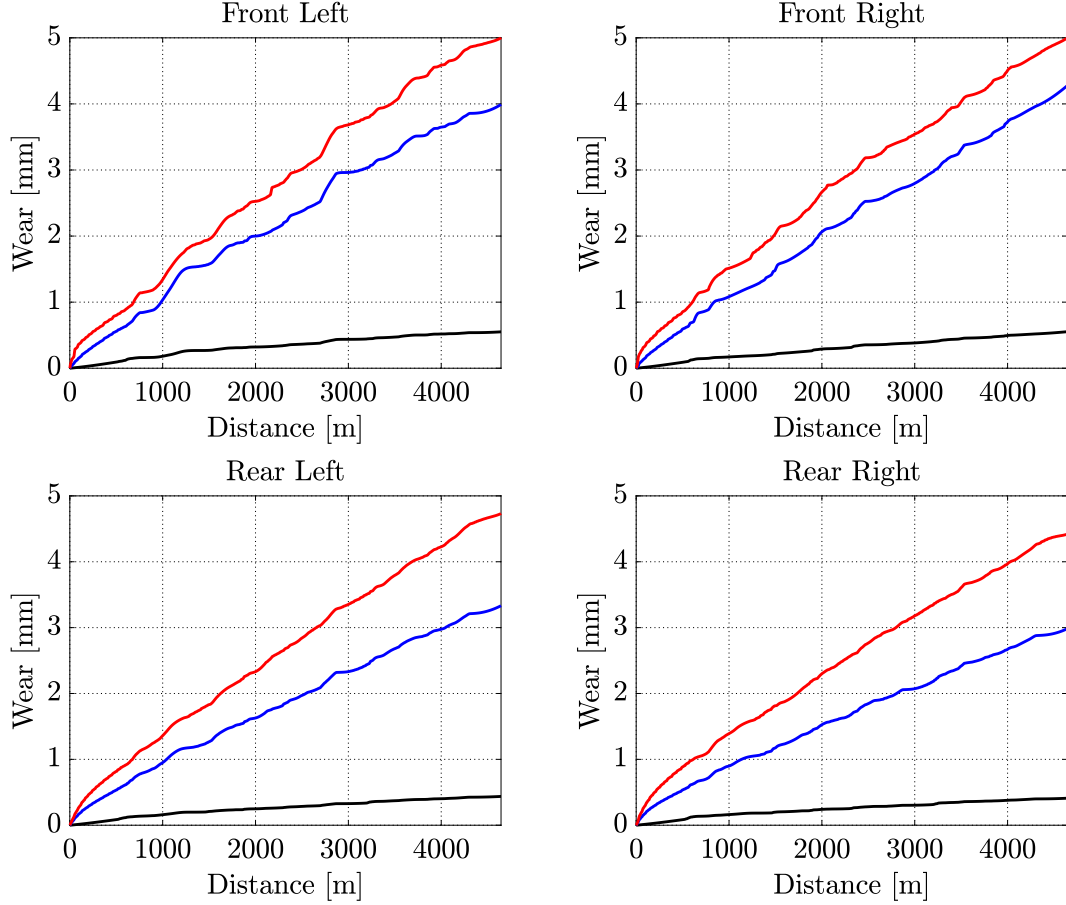**Figure 9.** Single-lap accelerated tyre wear. The nominal wear rate case is shown black, the ×10 nominal case is shown in blue, while the ×15 nominal case is red. Tyre heating effects are included.

4.3. Multi-lap simulation

In this simulation the tyre-wear model was adjusted back to its nominal wear rate to allow for multiple laps, with the results shown in Figure 10. Lap 2 is again the fastest lap. The slow first lap reflects the combined influence of cold new tyres that have not yet been 'rubbed in'. The tyres operate optimally between laps two and eight, with the lap times gradually increasing due to wear. After lap eight, tyre wear affects performance more noticeably, and the lap times start to degrade. At some point in the stint, this drop-off in performance increases to the extent that the car is no longer competitive and a tyre change is required. This performance drop-off is not seen in Figure 7, where tyre wear is unaccounted for, and the ΔT value reaches a steady-state value of approximately 0.1 s. When wear is accounted for, the lap ΔT continues to increase until the car is uncompetitive; see Figure 10(a). Figure 10(b) shows that the friction factor increases rapidly in the first lap when the tyres are being 'rubbed in'. After that they continue to wear with an accompanying reduction in the available friction. This wear-related degradation is most evident in the front-left tyre, which is down to 0.5 mm of tread at the end of the 15-lap stint. The front-right tyre is also well worn after 15 laps, with some life remaining in the rear tyres (approximately 2 mm of tread).
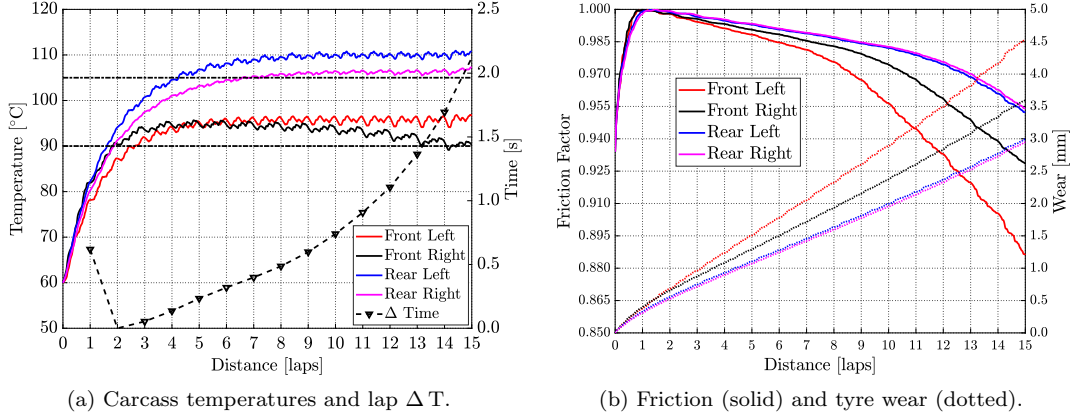
14

(a) Carcass temperatures and lap Δ T.

(b) Friction (solid) and tyre wear (dotted).

Figure 10. Carcass temperature and tyre degradation for a 15–lap racing stint.

4.4. Sensitivity study: track temperature

The concluding simulation illustrates the influence of track temperature variations on tyre performance. The first lap is a slow warm-up lap used to 'scrub in' the tyres and bring them up to their optimal operating temperature. The car speed is under $50 \, \mathrm{m/s}$ for most of the first lap; lap-time minimisation is only invoked for the second lap. Figure 11(a) shows the tread and carcass temperatures of all four tyres starting the slow lap at $60°C$; the track temperature is $10°C$. The tread temperatures rise quickly and are within the optimal operating band within a quarter of a lap. The carcass temperatures rise more slowly, but are close to their operating temperatures by the end of the warm-up lap. Figure 11(b) slows a rapid rise in the friction factor (from below 0.94) as the tyres are warmed and scrubbed in. By the end of the first lap the friction factors are all at approximately one, with a slight wear-related reduction evident thereafter. While cold, all four tyres wear rapidly during the first quarter lap. Figure 6 shows that tyre wear is a minimum at the graining-blistering transition temperature (of $100°C$ in this case). Thereafter they wear at approximately the same rate. During the high-speed second lap the tyres continue to wear with the front-left tyre wearing most rapidly. The tyres wear by less than $0.4 \, \mathrm{mm}$ during the first lap, the wear at the end of the second lap is under $0.8 \, \mathrm{mm}$.

Variations in the tyres' properties are now studied in response to changes in the track temperature; the tread and carcass temperatures again begin at $60°C$. Figure 12 shows the tyre temperature and wear for the rear-left tyre over a range of track temperatures. Figure 12(a) shows that on the second lap an increased track temperature cause marginal increases in the tread temperature, and a marginal reduction in the carcass temperature. This is predominantly the result of lower conduction losses to the track. On the basis of the Lap 2 carcass temperature profiles in Figure 12(a), one might expect that track temperature increases would lead to reduced tyre wear. Figure 12(b) shows that the total wear for the $50°C$ track temperature case is $\approx 0.67 \, \mathrm{mm}$; see the black dotted reference curve. The remaining curves in Figure 12(b) show that as the track temperature drops, the tyre tread wear increases by up to $0.06 \, \mathrm{mm}$ in the $0°C$ case.

15

(a) Car speed (dotted); carcass temperatures (dashed) tread temperatures (solid).

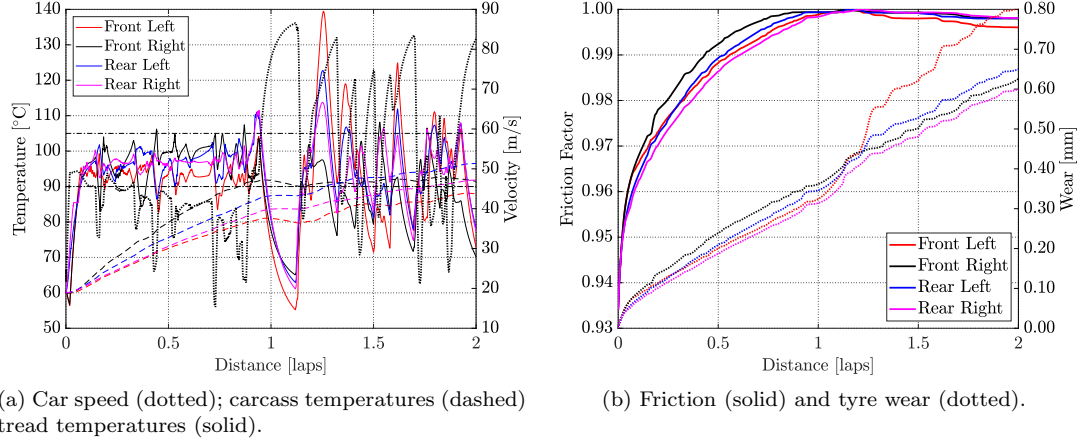(b) Friction (solid) and tyre wear (dotted).

Figure 11. Speed, and friction factors and wear for an ambient temperature of $25°$C and a track temperature of $10°$C. The wear curves are shown dotted.

(a) Tread (solid) and carcass (dashed) temperatures.

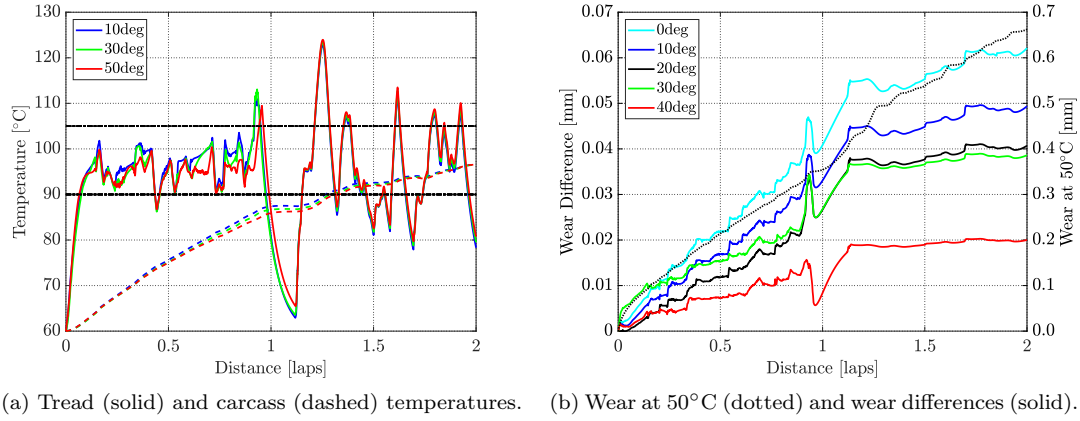(b) Wear at $50°$C (dotted) and wear differences (solid).

Figure 12. Rear-left tyre temperature and wear sensitivity to track temperature.

5. Track-side example

Tyre wear and temperature influences are central to the development of a practical tyre management strategy. On 8 September 2019, Charles Leclerc claimed victory for Ferrari in the Italian Grand Prix. Charles Leclerc, Lewis Hamilton and Valtteri Bottas changed places for the top three positions throughout the race. All three drivers started the race on the soft compound tyres, but opted for different strategies after their respective pit stops. The time differences for each driver relative to the leader of the race is shown in Figure 13. Mercedes implemented two strategies: (i) they pitted Hamilton nine laps before Bottas and fitted medium compound tyres; (ii) they pitted Bottas much later so that he would finish the race on fresher tyres. Ferrari pitted Leclerc immediately after Hamilton, but opted for hard compound tyres.

A combination of Ferrari's straight-line speed advantage, and the use of more durable hard-compound tyres helped them to victory. After lap twenty eight the gap between Bottas and Leclerc continued to decrease, because the medium compound tyres fitted to Bottas' car were faster (and newer) than the hard compound tyres on Leclerc's Ferrari. By lap forty one Hamilton's tyres had reached the end of their life, and he traded places with Bottas and dropped out of contention. Ferrari's strategy to
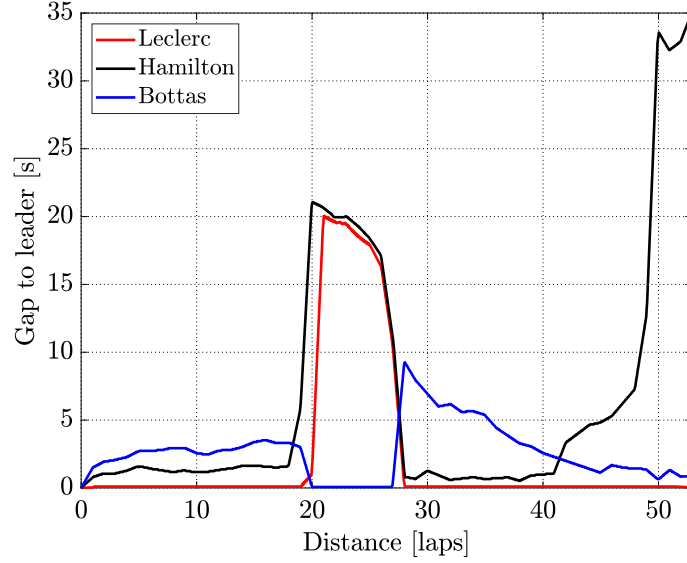
Figure 13. Gap to the race leader of the 2019 Italy Grand Prix—data accessed from [24].

go for a harder more durable compound put them in a position to compete for a world championship.

6. Conclusion

A thermodynamic tyre model is presented in which the tread and carcass temperatures are represented. The tyres' thermal behaviour impacts directly on their grip and wear properties; both are optimal within a narrow range of temperature. As the tyre wears, the peak friction reduces–the introduction of this wear-related grip feature is one of the novelties of this research. The tread temperature reacts rapidly to driver inputs and can be manipulated relatively easily into the optimal temperature window, where optimal grip is achieved. The carcass temperature, on the other hand, reacts more slowly, making it more difficult to manage. This is particularly true in cases where carcass-temperature reductions are required. By integrating the temperature-sensitive wear rate, it is possible to track accumulated tyre wear and its subsequent impact on the car's performance. Tyre wear is modelled as a function of tread temperature and the friction power generated in the tyres' contact region. Each tyre compound has its own unique friction and wear characteristics and will respond differently to wear. The model presented can be used to help determine the point at which tyre wear compromises performance to such an extent that the tyres are no longer viable. Increases in track temperature are found to result in reduced tyre wear (for the tyre data used here). Similar sensitivity studies could be carried out in much the same way. It is hoped that this study can be used to gain competitive advantage and improve tyre management strategies.

References

[1] Kelly DP, Sharp RS. Time-optimal control of the race car: influence of a thermodynamic tyre model. Vehicle System Dynamics. 2012 apr;50(4):641–662.

[2] Tremlett AJ, Limebeer DJN. Optimal tyre usage for a Formula One car. Vehicle System Dynamics. 2016 oct;54(10):1448–1473.

[3] Farroni F, Russo M, Russo R, et al. A physical-analytical model for a real-time local grip estimation of tyre rubber in sliding contact with road asperities. Proceedings of the Institution of Mechanical Engineers, Part D: Journal of Automobile Engineering. 2014 feb;228(8):955–969.

[4] Farroni F, Sakhnevych A, Timpone F. Physical modelling of tire wear for the analysis of the influence of thermal and frictional effects on vehicle performance. Proceedings of the Institution of Mechanical Engineers, Part L: Journal of Materials: Design and Applications. 2017 feb;231(1-2):151–161.

[5] Veirh AG. A review of important factors affecting treadwear. Rubber Chemistry and Technology. 1992;65(3):601–659.

[6] Muhr AH, Roberts AD. Rubber abrasion and wear. Wear. 1992;158:213–228.

[7] Schallamach A, Turner DM. The wear of slipping wheels. Wear. 1960;3:1–25.

[8] Gipser M. Ftire–the tire simulation model for all applications related to vehicle dynamics. Vehicle System Dynamics. 2007;45:139–151.

[9] Persson BNJ. Theory of rubber friction and contact mechanics. Journal of Chemical Physics. 2000;115(8):3840–3861.

[10] Schallamach A. Recent advances in knowledge of rubber friction and tire wear. Rubber Chemistry and Technology. 1968;41(1):209–244.

[11] Perantoni G, Limebeer DJN. Optimal control for a Formula One car with variable parameters. Vehicle System Dynamics. 2014 may;52(5):653–678.

[12] Limebeer DJN, Perantoni G, Rao AV. Optimal control of Formula One car energy recovery systems. International Journal of Control. 2014 oct;87(10):2065–2080.

[13] Limebeer DJN, Perantoni G. Optimal Control of a Formula One Car on a Three-Dimensional Track—Part 2: Optimal Control. Journal of Dynamic Systems, Measurement, and Control. 2015 may;137(5).

[14] Haney P. The Racing & High-performance Tire. SAE International and TV Motorsports; 2003.

[15] Mark JE, Erman B, Roland CM. The Science and Technology of Rubber Fourth Edition. Boston: Academic Press; 2013.

[16] Farroni F, Giordano D, Russo M, et al. TRT: thermo racing tyre a physical model to predict the tyre temperature distribution. Meccanica. 2014;49(3):707–723.

[17] Dyson FJ. A meeting with Enrico Fermi. Nature. 2004;427:297.

[18] Clark SK, Dodge RN. heat generation in aircraft tires. Computers and Structures. 1985; 20(1-3):535–544.

[19] Çengel Y, Cimbala J. Fluid mechanics - fundamentals and applications. McGraw-Hill; 2014.

[20] Limebeer DJN, Massaro M. Dynamics and Optimal Control of Road Vehicles. Oxford University Press; 2018.

[21] Pacejka H. Tire and Vehicle Dynamics. Elsevier Science; 2005.

[22] Betts JT. Practical methods for optimal control and estimation using nonlinear programming. 2nd ed. Society for Industrial and Applied Mathematics; 2009. Advances in Design and Control.

[23] Patterson MA, Rao AV. GPOPS-II: A MATLAB Software for Solving Multiple-Phase Optimal Control Problems Using hp-Adaptive Gaussian Quadrature Collocation Methods and Sparse Nonlinear Programming. ACM Trans Math Softw. 2014 oct;41(1):1:1—-1:37.

[24] Collantine Media Ltd. 2019 Italian GP interactive F1 lap charts, times and tyres — Race-Fans ; 2019. Available from: https://www.racefans.net/2019/09/08/2019-italian-grand-prix-interactive-data-lap-charts-times-and-tyres/.